SINGLE BREATH-HOLD RENAL T1 IMAGING AT 7T

Xiufeng Li[1], Patrick J. Bolan[1], Kamil Ugurbil[1], and Gregory J. Metzger[1]
[1]*Center for Magnetic Resonance Research, University of Minnesota, Minneapolis, MN, United States*

Introduction: Knowledge of renal tissue's longitudinal magnetization relaxation time, T_1, which changes with the field strength, is essential in renal imaging protocol optimization for appropriate image contrast and quantitative non-contrast enhanced renal perfusion imaging using arterial spin labeling at 7T (1). Previous studies have indicated that, compared to T_2 and spin density, the longitudinal relaxation time can be more important in characterizing renal diseases (2-3) and differentiating specific disease states (4). In this study, renal longitudinal relaxation times were measured in healthy normal volunteers within a single breath-hold by using single-shot fast spin echo (ss-FSE) with varied inversion recovery times (5). The reproducibility of renal T_1 mapping was also evaluated with repeated studies in two sessions approximately one week apart. To our knowledge, these are the first renal T_1 measurements in human at 7T.

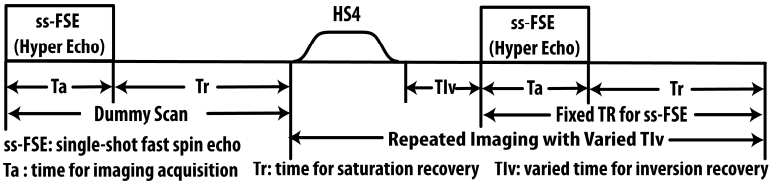

Figure 1. Sequence diagram for renal T_1 imaging.

Materials and Methods: All healthy volunteers provided written informed consent prior to being studied according to a local IRB approved protocol: six subjects (five males: 49 ± 19 years, mean ± SD and one female: 21 years) participated in renal T_1 imaging. The five male subjects also took part in a second imaging session (about one week later) for the evaluation of the reproducibility of renal T_1 measurements. Studies were performed on a Siemens 7T whole body MRI scanner with an external 16-channel transceiver TEM stripline array driven by a series of 16, 1 kW amplifiers (CPC, Pittsburgh, PA). To minimize B_1+ inhomogeneity across the kidney region and reduce RF power deposition, one side of the kidneys was selected for imaging. B_1+ optimization was performed in the selected kidney region by using tradeoff B_1+ shimming solution (6), and local B_0 optimization was achieved by using volumetric phase maps acquired within a single breath-hold (7). The RF reference voltage was adjusted based on the calibrated B_1+ estimation from a 2D single slice *actual flip angle imaging* (8) measurement acquired within a single breath-hold. An adiabatic HS4 RF pulse was used for slice selective inversion with a slab size two times larger than imaging slice thickness. For each subject, T_1 imaging was performed with both the calibrated RF reference voltage and with the voltage increased 8 to 12 % to verify that the power was calibrated sufficiently to achieve adiabaticity for the slice-selective inversion. A ss-FSE imaging sequence using hyper echoes (Figure 1) was used for T_1 mapping. Both the ss-FSE and the B_1+ calibration method were evaluated with phantom studies prior to in vivo imaging. ss-FSE imaging parameters were: TR/TE = 3.0-4.0 s/ 16 ms, FOV = 192 x 192 mm^2, in-plane resolution = 1.5 x 1.5 mm, slice thickness = 5 mm, phase encoding direction = anterior to posterior with 50% oversampling, partial Fourier = 5/8, parallel imaging acceleration factor = 4 with separately acquired 24 reference lines, hyper echo flip angle = 90 degree. To further minimize short-term specific absorption rate (SAR), the inversion times for the six measurements were arranged in the following order: 0.1, 1.2, 0.15, 0.8, 0.3 and 0.5 s.

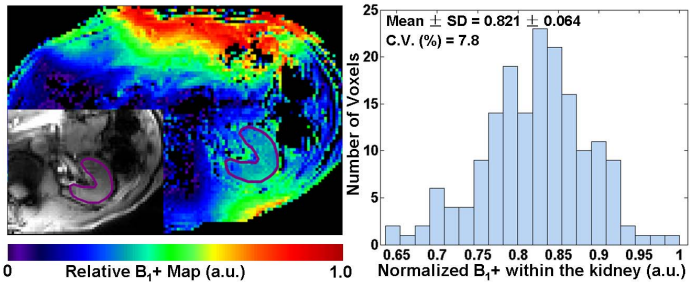

Figure 2. B_1+ map and distribution within the kidney from one typical subject. GRE image with overlaid ROI is also presented for further reference.

Nonlinear least square model fitting was performed in Matlab for images acquired at different inversion times with the following equation (5):

$$S = \sqrt{[S_0 \cdot (1 - 2 \cdot \exp^{-TI_v/T_1} + \exp^{-T_r/T_1})]^2 + C_{noise}^2}$$

where S is measured signal intensity, S_0 proton density weighted by coil sensitivity and imaging gain, and C_{noise} estimated imaging noise. ROIs for renal cortex and medulla were conservatively defined by using images acquired around the nulling point as the reference. To minimize partial volume effects and errors due to physiological noise, a trimmed mean was used for T_1 estimation, excluding the 5% of voxels with the lowest values and the 5% with the highest values based on the histogram from each ROI.

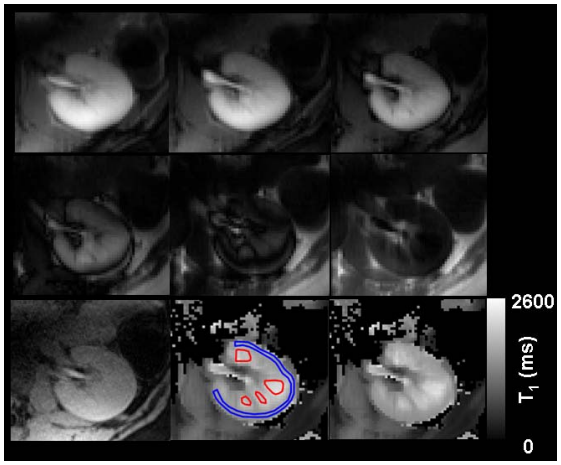

Figure 3. One subject's ss-FSE images acquired with six inversion times (0.1 to 1.2 s from the top left to middle right), anatomic GRE image (bottom left) and T_1 maps with/without overlaid ROIs for the cortex (blue) and medulla (red).

Results and Discussion: By properly balancing B_1+ inhomogeneity and RF efficiency in the kidney region and with the consideration of short-term SAR limitation, B_1+ optimization was effectively performed for reliable renal T_1 imaging across all subjects. A representative example is given in Figure 2. We verified that the B1+ calibration was correct by noting: 1) that scans acquired with the higher HS4 RF voltage did not significantly change renal T_1 measurements (data not shown); and 2) that no signiciant differences were found between T_1 measurements in regions with high and low B_1+ amplitudes (data not shown). ss-FSE images and a renal T_1 map from a typical subject are shown in Figure 3. Estimated T_1s for renal cortex and medulla were 1639.0 ± 99.1 ms and 2085.6 ± 81.1 ms (mean ± SD) respectively (Figure 4, left). The reproducibility study showed small percentage differences across two sessions: 1.7±4.9% for cortical T_1 and -0.8±3.5% for medullary T_1 (Figure 4, right).

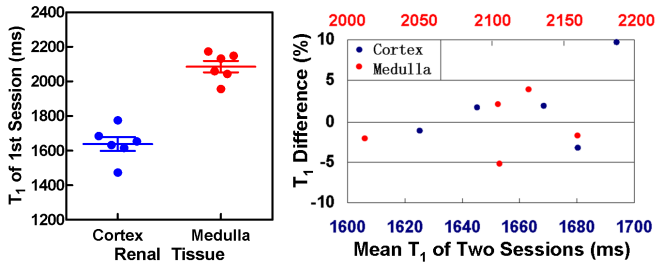

Figure 4. Renal T_1 measurements from the first session (N = 6) (left) and Bland–Altman plots (right) showing the percent differences between renal T_1 measurements across two sessions (N=5). Error bars represent standard errors.

Conclusions: Renal longitudinal relaxation times can be reliably and reproducibly measured by using ss-FSE with varied inversion times within a single breath-hold at 7T.

Acknowledgements: Funding Provided by P41 EB015894, S10 RR026783 and WM KECK Foundation.

References: 1. Li et al., Proc. ISMRM 2012;1310. **2.** Terrier et al., Eur J Radiol 1986;6:121–126. **3.** Semelka et al., Radiology 1994;190:149–152. **4.** Lee et al., JMRI 2007;25:790–795. **5.** de Bazelaire et al., Radiology 2004;230(3):652-659. **6.** Metzger et al., MRM 2012 (online in press). **7.** Shah et al., Proc. ISMRM 2009:566. **8.** Yarnykh et al., MRM 2007;57(1):192-200.